Int J Clin Exp Med 2019;12(12):13325-13336
www.ijcem.com /ISSN:1940-5901/IJCEM0102774

Original Article

The effects of mesenchymal stem cell exosome with an overexpression of miR-148a on hepatic ischemia-reperfusion injury

Kate Nong, Shengyong Liu, Dong Zhang, Changze Chen, Yong Yang, Yue Yang, Huihua Cai

Department of Hepatobiliary Surgery, The First People's Hospital of Changzhou, The Third Affiliated Hospital of Soochow University, Changzhou 213000, Jiangsu, China

Received September 25, 2019; Accepted November 8, 2019; Epub December 15, 2019; Published December 30, 2019

Abstract: Purpose: This study aimed to investigate the effect of the overexpression of miR-148a in mesenchymal stem cell exosomes on hepatic ischemia-reperfusion (I/R). Methods: Fat MSCs were extracted from the fat tissue around the kidneys of rats. Lentivirus-infected MSC cells loaded with an miR-148a overexpression sequence or an unrelated sequence vector were used to extract the over-expressed sequence, the unrelated sequence, and the normal MSC exosome cells. The perihepatic ligament was broken in the sham operation group, and no other treatment was performed. The model group was not injected with the exosome solution. The experiment group was injected via the tail vein with transfected exosomes with miR-148a overexpression. The expressions of miR-148a, TLR4 mRNA, and CaMKII mRNA in the liver tissues were determined using RT-qPCR. All the rats' liver tissues were observed after the HE staining, and the apoptosis of the liver cells was tested using TUNEL. The expressions of the TLR4, CaMKII, Bcl-2, and Bax proteins in the liver tissues were determined using Western blot. ELISA was used to determine the expressions of IL-1β and TNF-α in the serum. The TargetScan prediction and dual-luciferase reporter system were used to identify the relationship between miR-148a and CaMKII. Results: The MSC and the exosomes were successfully extracted and identified. The miR-148a in the overexpression group was significantly higher than it was in the other groups ($P<0.05$). The TLR4, CaMKII mRNA, and protein in the overexpression group were significantly lower than they were in the model and experimental groups ($P<0.05$). The TargetScan and dual-luciferase reporter system confirmed the targeted regulation relationship between miR-148a and CaMKII. Conclusion: The overexpression of miR-148a in mesenchymal stem cell exosomes can inhibit the expressions of CaMKII and TLR4 in I/R tissues and reduce the occurrence of the inflammatory response and apoptosis.

Keywords: miR-148a, mesenchymal stem cells, exosomes, hepatic ischemia-reperfusion injury

Introduction

In clinical liver surgery, in order to control blood loss, the porta hepatis should be blocked. Then ischemia/reperfusion (I/R) injury becomes inevitable when the liver blood supply is restored, which is common in traumatic shock and liver transplantation [1, 2]. One study has shown that [3] early liver I/R injury can cause the inflammatory response and an oxidative stress reaction, accelerate hepatocyte apoptosis and necrosis, and then induce liver function damage or insufficiency. In addition, after hepatocyte injury, a large number of pro-inflammatory factors will then be released, which will promote the activation of the inflammatory response to cause a vicious circle and liver function damage [4]. Therefore, how to reduce and prevent the occurrence of I/R is an urgent problem for clinicians.

A research hotspot in recent years, mesenchymal stem cells (MSC) are adult hepatocytes which can be multi-directionally differentiated into cells such as osteogenesis and fat. Studies have shown that MSCs have therapeutic effects in various diseases such as immune diseases, cardiovascular diseases, and tissue damage diseases [5-7]. The mechanism of MSC treatment mainly includes homing and repairing damaged tissues, secreting vascular growth factors, activating in vivo stem cells, and secreting

exosomes [8]. Wang et al. showed that spherical cultured human umbilical cord mesenchymal stem cells can alleviate liver ischemia-reperfusion injury in rats [9].

Some studies [10, 11] have shown that the therapeutic effects of MSCs are closely related to exosomes. Exosomes are vesicular bodies released by cells, which have a lipid bilayer membrane with a diameter of 40~100 nm [12]. A study found hepatocyte-derived exosomes could aid cell proliferation and liver regeneration after ischemia/reperfusion injury [13].

A certain amount of miR (microRNA) and other regulating materials are also present. miR is a non-coding, short interfering RNA with a length of about 22 nt. It plays a major role by combing the untranslated regions (UTR) of its downstream target gene mRNA. Thereby, the translation and transcription of target genes are inhibited and the expressions of the target genes are altered [14, 15]. miR-148a is an important member of the miR family. Related studies have shown [16, 17] that it is differentially expressed in various tumors, and miR-148a may mitigate hepatic I/R injury by ameliorating TLR4-mediated inflammation by targeting CaMKIIα in vitro and in vivo [18].

CaMKIIα (Ca^{2+}/calmodulin-dependent protein kinase IIα), also known as CaMKII, is an important factor for regulating the Ca^{2+}/CaMKII and TLR4 signaling pathways. A study by Vila et al. [19] showed that the inhibition of CaMKII can protect irreversible ischemia-reperfusion injury. We found that there is a targeted binding site between miR-148a and CaMKII using TargetScan database. We speculate that they are closely related.

Therefore, this study investigated the effects of the overexpression of miR-148a in MSC exosomes on hepatic ischemia-reperfusion (I/R).

Materials and methods

Animal and cell sources

293T human embryonic kidney cells were purchased from the ATCC Company (ATCC® ACS-4500). 43 SPF male SD rats, 6 weeks old and weighing 175±25 g were purchased from the Beijing Charles River Experimental Animal Technology Co., Ltd. The animal certificate number is SCXK (Jing) 2015-0001. After purchasing the rats, they were kept in the standard breeding room of the animal research center of the hospital for 1 week. The room temperature was 22~26°C, and the relative humidity was 50%~65%, with a 12-hour light-dark cycle.

Instrument reagent sources

Chloral hydrate (American Sigma, 47335-U), a dual-luciferase reporter gene detection kit (Solarbio, Beijing, China D0010), fetal bovine serum (FBS), trypsin, PBS, TRIzol™ Reagent, an ECL luminescence detection Kit, a Lipofect-AMINE 2000 kit, RIPA, a BCA protein kit, type I collagenase, (American Thermo Scientific, 10-437028, A40007, 10010049, 15596018, 35-050, 11668019, 23225, 15224041, 12320-032, 17018029), DMEM low sugar medium, α-MEM medium, penicillin streptomycin double antibody (Hyclone, USA, 12320032, 12561049, 15070063), TransScript Green miRNA Two-Step qRT-PCR SuperMix, TransScript II Green Two-Step qRT-PCR SuperMix (Beijing, China, TransGen Biotech, AQ202-01, AQ301-01), NL-R4 (Toll-like Receptor 4) Antibody, CaMKII Antibody, Bcl-2 Antibody, Bax Antibody, β-Actin, HRP-labeled goat anti-mouse IgG secondary antibody (AF5015, MAB7280, AF810, AF820, MAB8929, HAF007, R&D, USA), IL-1β, TNF-α Elisa kit (Beyotime Biotechnology, Shanghai, China), Chemistry, PI301, PT512), a PCR instrument (ABI, USA 7500), flow cytometry (FACS Canto II, BD, USA), a microplate reader (Perkin-Elmer, USA BioTek), an miR-148a lentiviral vector, and an unrelated sequence vector and related primers designed and synthesized by Shanghai Jemma Biotechnology Co., Ltd.

Cell collection and culture

About 1 mg of adipose tissue around the rat kidney was collected, and the tissue was cut into pieces using surgical scissors, and the pieces were immersed in type I collagenase (5 mL) at 37°C for 60 min. The tissue was shaken and centrifuged at 1300 rpm for 5 min. The collected cells were transferred to a DMEM low glucose medium containing penicillin streptomycin diabody, 10% FBS, cultured at 37°C, 5% CO_2, observed every 12 h. We cultivated the next generation when the cells covered the bottom of the bottle, and the liquid was changed every 3 days.

Cell identification

The P3 generation cells were collected by flow cytometry, and the cell surface markers CD29, CD44, CD73, CD90, and CD105 were identified. The cells were cultured with osteoblasts and adipocytes, and the fat cells were identified using red oil staining. The bone cells were determined with Alizarin staining.

Cell transfection

The over-expressed miR-148a-mimic vector and the unrelated sequence lentiviral vector were transfected into the corresponding fat MSC cells, Lentiviral transfection was performed using the LipofectAMINE 3000 kit. The medium was replaced after 24 hours. After 72 hours, the number of fluorecyte cells was observed. 1 mg/L of puromycin was used to screen the positive cells, so the stable over-expressed miR-148a-mimic and unrelated sequence fat MSC cells were obtained.

Extraction and identification of exosomes

The collected transfected and untransfected fat MSC cells were cultured for 48 h, and the supernatant was collected after 48 h. The cells were centrifuged at 2000 rpm, at 4°C for 10 min. The bottom cells were transferred to a centrifuge tube, and then centrifuged at 4000 rpm for 10 min at 4°C. Then the bottom cells were collected and resuspended in PBS, centrifuged at 10,000 rpm, 4°C for 30 min at 4°C. The bottom layer cells were again collected, centrifuged at 30,000 rpm 4°C for 1.2 h, and then the collected cells (the exosomes) were resuspended in 200 μL of PBS, and the morphology of the cells was observed using an electron microscope.

Establishment of the animal models

Rats were fasted 12 hours before surgery and intraperitoneally injected with 10% chloral hydrate at 2.5 mL/kg. Sevoflurane was delivered to the chamber at a rate of 2-3 L/min in a humidified 30% oxygen carrier gas. During the laparotomy, the rats were placed on a heating pad and the light was maintained at 37°C to ensure an aseptic operation. Heparin (125 IU/kg) was injected intravenously to prevent the formation of a portal vein pool. The vascular microclamps were placed in the medial and left hepatic hila for 45 min to induce hepatic ischemia in the rats. The color of the left hepatic lobe became shallow, indicating that the experiment was successful. The animals in the sham operation group only received anesthesia, and no vascular microclamps were used in the laparotomy. After 45 minutes, the blood vessel clamp was removed, and saline was injected intraperitoneally, and the rats were sutured. The exosome solution (500 μg of exosomes dissolved in 1 mL of PBS solution) was injected into the tail vein 24 hours before the surgery. No animal model was established in the normal group. The perihepatic ligament was broken in the sham operation group and no other treatment was performed. The model group was not injected with the exosome solution. The experiment group was injected with PBS. The blank group was treated with an exosome solution transfected using a blank vector, and the overexpression group was injected with an exosome solution transfected with an overexpression vector. 12 hours after the establishment of the model, the rats were sacrificed using either anesthesia or the air embolization method, and then the rat liver tissues and vena cava blood were collected for the post-study test.

Determination of the miR-148a, NLR4, and CaMKII expressions in the rat liver tissue

HE staining: Liver tissues fixed in 4% formalin at 4°C for 48 h were embedded in paraffin blocks and sliced at a thickness of 4 μm. The slices were subject to gradient dehydration with ethanol (100% for 10 min, 95% for 10 min and 80% for 10 min), and dewaxed in dimethylbenzene. After the HE staining was done according to standard procedures (21), the tissues were observed under an optical microscope for pathological changes and magnified 200X to observe the cellular morphology.

The total RNA of the collected liver tissue was extracted with a TRIzol kit. The purity, concentration, and integrity of the total extracted RNA were determined using an ultraviolet spectrophotometer and agarose gel electrophoresis. The miR-148a determination method was as follows: Reverse transcription of the total RNA was performed using TransScript® miRNA RT Enzyme Mix and 2× TS miRNA Reaction Mix. The procedure was carried out in strict accordance with the manufacturer's instructions.

Table 1. Primer sequence

Gene	Upstream primer	Downstream primer
miR-148a	5'-GTAAGTGCCTGCATGTATATG-3'	5'-TACGTGTCGTGGAGT-3'
TLR4	5'-GGGTCAAGGAACAGAAGCA-3'	5'-TGAAGGCAGAGGTGAAAGC-3'
CaMKII	5'-TTTGGATTTGCGGGAACAC-3'	5'-TGACTCCGTCTGCTTTCTT-3'
U6	5'-CTCGCTTCGGCAGCACA-3'	5'-AACGCTTCACGAATTTGCGT-3'
GAPDH	5'-AAGAAGGTGGTGAAGCAGGC-3'	5'-TCCACCACCCTGTTGCTGTA-3'

Then the PCR amplification experiments were performed. The PCR reaction system included: 1 μL of cDNA, 0.4 μL of upstream and downstream primers, 2× TransTaq® Tip Green qPCR SuperMix, and 10 μL and 0.4 μL of Passive Reference Dye (50×) were added to ddH_2O until 20 μL. The PCR reaction conditions: pre-denaturation at 94°C for 30 s, denaturation at 94°C for 5 s and annealing at 60°C for 30 s. It was 40 cycles in total. 3 replicate wells were set for each sample, and the experiment was performed 3 times. In this study, U6 was used as an internal reference for miR-148a, and $2^{-\Delta\Delta ct}$ was used to analyze the data. The detection program of NLR4 and CaMKII was as follows with GAPDH as the internal control: the reverse transcription was performed using the 5× TransScript® II All-in-One SpuperMix for qPCR and gDNA Remover kits. The procedure was carried out in strict accordance with the manufacturer's instructions. **Table 1** lists the primer sequences.

Apoptosis testing by TUNEL: The liver tissues were fixed with 10% paraformaldehyde, embedded in paraffin, and sliced at a thickness of 4 μm to test the apoptosis using the TUNEL kits (terminal deoxynucleotidyl transferase (TdT)-mediated dUTP Nick End Labeling) (Roche, Switzerland) according to the instructions. The cellular nuclei with a positive TUNEL result were yellowish-brown, and chromatin aggregation or chromatorhexis can be seen under a high power lens.

Determination of the NLR4, CaMKII, Bcl-2, and Bax protein expressions in the rat liver tissue

The total protein of the collected liver tissue was extracted using the RIPA pyrolysis method. The protein concentration was calculated using the BCA method. The protein concentration was adjusted to 4 μg/μL and separated using 12% SDS-PAGE electrophoresis. After ionization, the membrane was transferred to a PVDF membrane. It was stained with a ponceau working solution and immersed in PBST for 5 min. 5% skim milk powder was used to block it for 2 h. NLR4, CaMKII, Bcl-2, and Bax primary antibodies (1:1000) were added at 4°C and the solution was kept overnight. The primary antibody was removed by washing the membrane. Horseradish peroxidase-labeled goat anti-mouse secondary antibody (1:5000) was added. Then it was incubated at 37°C for 1 h and rinsed 3 times with PBS for 5 min in each time. It was developed in a dark room. Filter paper was used to absorb the excess liquid on the membrane. The ECL was illuminated and developed. The protein bands were scanned, and the gray values were analyzed using Quantity One software. The relative expression level of the protein = the gray value of the target protein band/the gray value of the β-Actin protein band.

The expressions of the IL-1β and TNF-α inflammatory factors in rat serum

The serum was collected by centrifuging the rat vena cava blood at 3000 rpm and 25°C for 10 min. The kit was used for quantification. The specific program was as follows: 50 μl of different concentrations of the standard solution were added to the blank micro-wells; 50 μl of distilled water and 50 μL of antibody were added into the blank control wells; 40 μl of the sample and then 10 μl of the biotin-labeled antibody were added to the remaining micro-wells, then they were incubated at 37°C for 30 min. The washing solution in each well was ensured to be full without overflowing for 30 seconds. Then it was patted dry 5 times. 50 ul of the enzyme-labeled solution was added to each well, then incubated at 37°C for 60 min. The plate was washed again 5 times. The absorbent paper was used to dry it thoroughly. Horseradish peroxidase was added to mark the 100 μl/well. It was incubated at 37°C for 15 min in the dark. Chromogenic substrate TMB in a 100 μl/well was added and incubated at room temperature for 20 min in the dark. Finally, 50 μl/well of the stop solution was added. The microplate reader was used to determine the maximum absorption wavelength

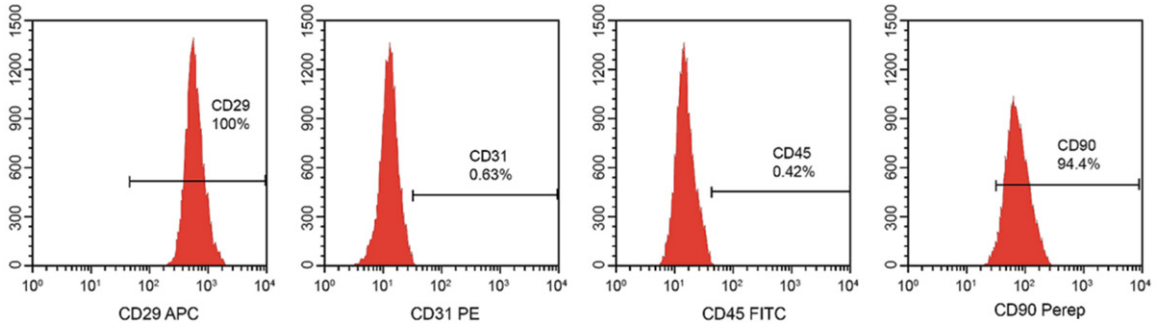

Figure 1. CD29, CD31, CD45, CD90 identification of MSC cells.

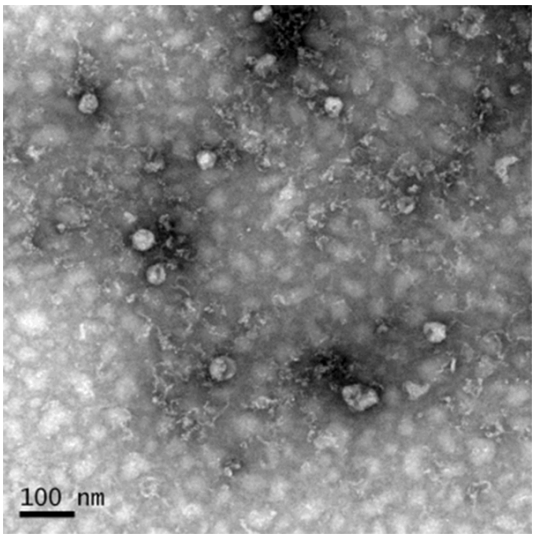

Figure 2. Exosomes under an electron microscope.

at 450 nm within 15 min. 3 sets of duplicate wells were set, and the experiment was repeated 3 times.

TargetScan target gene prediction and dual-luciferase reporter system

The TargetScan database was applied to predict the target gene of miR-148a. The CaMKII gene was constructed using the miR-148a-mimic and a blank sequence. The recombinant psi-CHECK-2-CaMKII-WT plasmid and mutant psi-CHECK-2-CaMKII-MUT plasmid were transfected into 293T cells, which were adopted after 48 hours. The dual-luciferase reporter gene detection kit was used for the operation. Finally, the collected cells were quantified using a chemiluminescence microplate reader. 3 sets of duplicate wells were set and the experiment was repeated 3 times.

Statistical analysis

In this study, SPSS 20.0 software was used to analyze the collected data, and the relevant pictures were drawn with GraphPad Prism 7 software. KS was used to analyze the data distributions. Comparisons among groups were performed using a one-way analysis of variance and indicated by F. An LSD-*t* test was adopted for pairwise comparisons. $P<0.05$ meant there was a significant statistical difference.

Results

Identification of the fat MSC cells

By observing the fat MSCs of the primary rats under the microscope, it was found that the cells were spindle-shaped and slender, and they grew in a spiral shape. By detecting the cell surface CD markers, the MSC cell markers CD29 and CD90 were found to be positive, but the MSC hematopoietic markers CD31 and CD45 were found to be negative. The Alizarin Red staining and red oil staining demonstrated the osteogenic and fat differentiation capacities of the hepatocytes (**Figure 1**).

Exosome identification

The extracted exosomes were observed using electron microscopy. It revealed that the exosomes were about 50-100 nm under the electron microscope. The cells had a circular and elliptical cell vesicle structure (**Figure 2**).

Rat modeling

By hematoxylin-eosin staining (HE Staining), the normal group and the pseudo-operation group were found to have normally structured

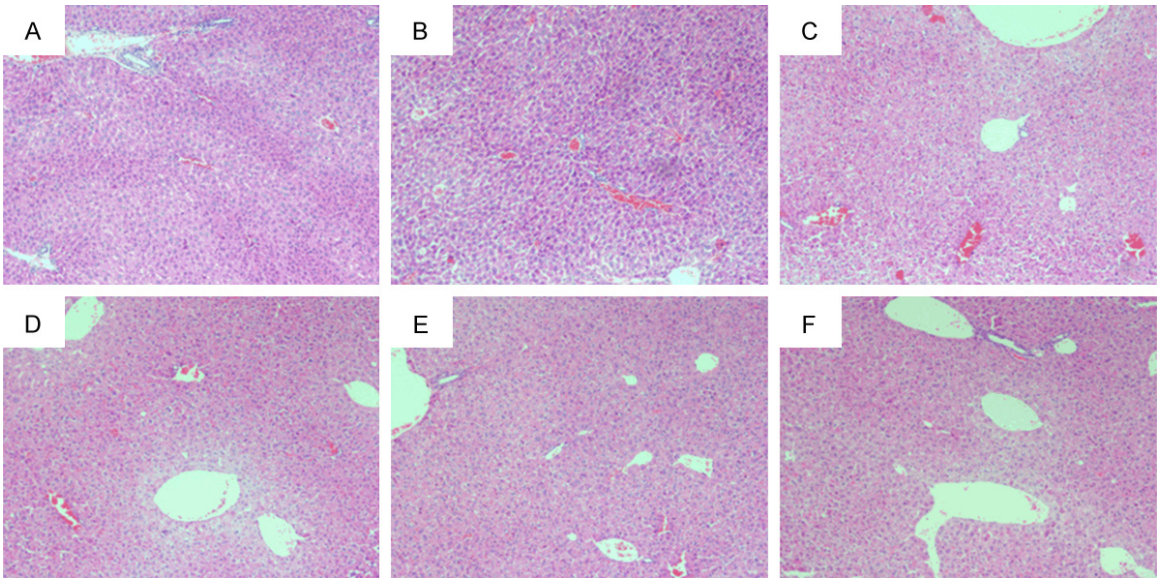

Figure 3. HE staining. A. HE stained liver tissue in the normal group. B. HE stained liver tissue in the sham operation group. C. HE stained liver tissue in the model group. D. HE stained liver tissue in the experimental group. E. HE stained liver tissue in the blank group. F. HE stained liver tissue in the overexpression group.

liver tissues and normally shaped liver cells, intact acini hepatis, and neatly arranged hepatic sinusoids, without any significant necrosis of the liver cells, inflammatory cell infiltration, bleeding, or swelling. The model group showed hydropic pathologies of degeneration and necrosis in many liver cells, a damaged acini hepatis structure accompanied by inflammatory cell infiltration, congested and swollen hepatic sinusoids in disorder; the blank group and the experiment group demonstrated a reduction in the hydropic pathologies of degeneration and necrosis in the liver cells, alleviated inflammatory cell infiltration, and swelling of the hepatic sinusoids, and such improvements were more dominant in the overexpression group (**Figure 3**).

Testing of I/R-related hepatic apoptosis by TUNEL

TUNEL was adopted to test the apoptosis in each group. In the model group, prominent hepatic apoptosis and karyopyknosis were observed when compared with the normal group and the pseudo-operation group, but in the blank group and the experiment group when compared with the model group, and in the overexpression group when compared with the blank group and the experiment group, the hepatic apoptosis and karyopyknosis were less significant (**Figure 4**).

Expressions of the inflammatory factors in the rat serum

The serum IL-1β and TNF-α expressions were significantly different among the groups ($P<0.05$). There was no significant difference in serum IL-1β and TNF-α expressions between the sham operation group and the normal group ($P>0.05$). There was no statistical difference in serum IL-1β and TNF-α expressions between the experimental group and the blank group ($P>0.05$). The expressions of IL-1β and TNF-α in the model group, the experimental group, the blank group, and the overexpression group were significantly higher than those of the normal group and the sham operation group ($P<0.05$). The expressions of IL-1β and TNF-α in the overexpression group serum were significantly lower than they were in the model group, the experimental group and the blank group ($P<0.05$). The expressions of IL-1β and TNF-α in the experimental group and the blank group were lower than they were in the model group ($P<0.05$) (**Table 2**).

The expressions of miR-148a, TLR4 mRNA, and CaMKII mRNA in liver tissue

The expressions of miR-148a, TLR4 mRNA, and CaMKII mRNA in the rats' liver tissues were significantly different among the groups ($P<0.05$). There was no difference in the expressions of

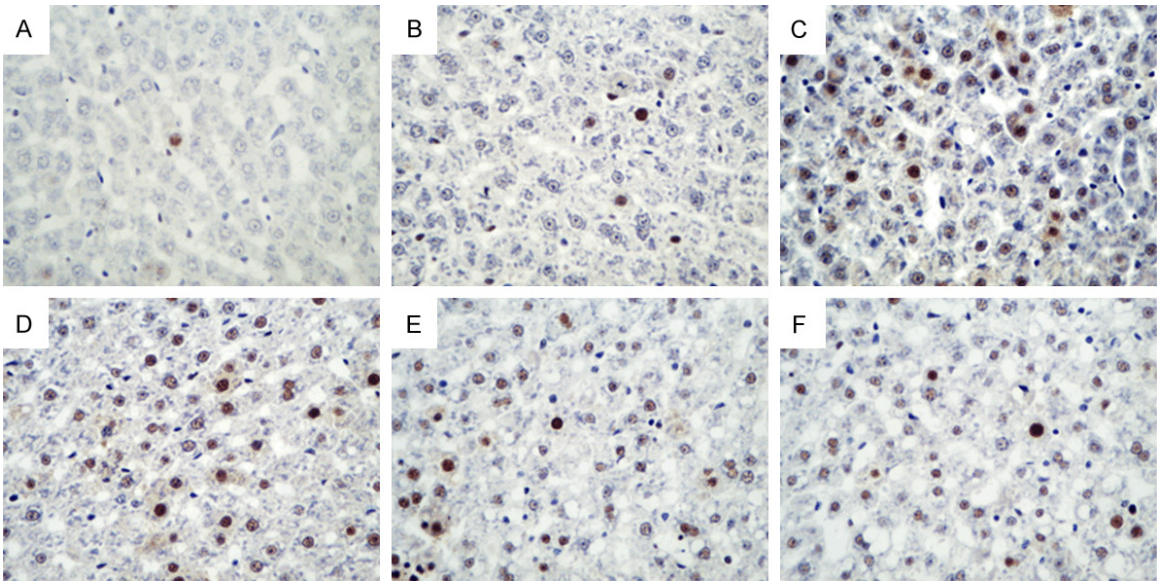

Figure 4. Apoptosis by TUNEL A. Apoptosis of liver tissue in the normal group. B. Apoptosis of liver tissue in the sham operation group. C. Apoptosis of liver tissue in the model group. D. Apoptosis of liver tissue in the experimental group. E. Apoptosis of liver tissue in the blank group. F. Apoptosis of liver tissue in the overexpression group.

Table 2. The expressions of IL-1 β and TNF-α in the serum of rats

Group	IL-1β (ng/L)	TNF-α (ng/L)
Normal group (n=7)	16.45±4.84	18.44±3.11
Sham operation group (n=7)	18.39±5.24	20.15±4.73
Model group (n=7)	89.42±9.11$^{*,\#}$	189.18±15.70$^{*,\#}$
Experimental group (n=7)	62.17±6.77$^{*,\#,\Delta}$	157.84±10.19$^{*,\#,\Delta}$
Blank group (n=7)	58.29±5.39$^{*,\#,\Delta}$	154.11±8.74$^{*,\#,\Delta}$
Overexpression group (n=7)	39.72±4.89$^{*,\#,\Delta,\triangledown,\blacktriangle}$	112.33±8.99$^{*,\#,\Delta,\triangledown,\blacktriangle}$
F value	142.997	419.627
P value	<0.001	<0.001

Note: *indicates there is a difference compared with the normal group (P<0.05), # indicates there is a difference compared with the sham operation group (P<0.05), $^{\Delta}$indicates there is a difference compared with the model group (P<0.05), $^{\triangledown}$indicates there is a difference compared with the experimental group (P<0.05), and $^{\blacktriangle}$indicates there a difference compared with the blank group (P<0.05).

miR-148a, TLR4 mRNA, and CaMKII mRNA between the sham operation group and the normal group (P<0.05). There was no difference in the expressions of miR-148a, TLR4 mRNA, and CaMKII mRNA between the experimental group and the blank group (P<0.05). The miR-148a expression in the liver tissue of the model group was significantly lower than of its expression in the normal group, the sham operation group, the experimental group, and the blank group. The CaMKII mRNA and TLR4 mRNA expressions in the liver tissue of the model group were significantly higher than they were in the normal group, the sham operation group, the experimental group, and the blank group (P<0.05). The miR-148a expression in the liver tissue of the overexpression group was significantly higher than it was in the other groups. The expressions of TLR4 mRNA and CaMKII mRNA in the overexpression group were lower than they were in the model group, the experimental group, and the blank group, but they were higher than they were in the normal group and the sham operation group (P<0.05). The miR-148a expression in the liver tissue of the experimental group and the blank group was higher than it was in the model group. The TLR4 mRNA and CaMKII mRNA expressions in the experimental group and the blank group were lower than they were in the model group (P<0.05) (**Table 3**).

The expressions of TLR4, CaMKII, Bcl-2 and Bax proteins in the liver tissue

The expressions of the TLR4, CaMKII, Bcl-2, and Bax proteins in the rats' liver tissues we-

Table 3. The expressions of miR-148a, TLR4 mRNA, and CaMKII mRNA in liver tissue

Group	miR-148a	TLR4 mRNA	CaMKII mRNA
Normal group (n=7)	1.012±0.045	1.025±0.064	1.033±0.069
Sham operation group (n=7)	1.032±0.061	1.039±0.071	1.038±0.077
Model group (n=7)	0.344±0.124*	1.844±0.388*	1.721±0.182*
Experimental group (n=7)	0.698±0.168$^{*,\#}$	1.612±0.225$^{*,\#}$	1.557±0.150$^{*,\#}$
Blank group (n=7)	0.725±0.184$^{*,\#}$	1.598±0.189$^{*,\#}$	1.530±0.180$^{*,\#}$
Overexpression group (n=7)	1.422±0.247$^{*,\#,\Delta,\triangledown,\blacktriangle}$	1.272±0.122$^{*,\#,\Delta,\triangledown,\blacktriangle}$	1.258±0.113$^{*,\#,\Delta,\triangledown,\blacktriangle}$
F value	39.514	18.306	31.568
P value	<0.001	<0.001	<0.001

Note: *indicates there is a difference compared with the normal group (P<0.05), $^{\#}$indicates there is a difference compared with the sham operation group (P<0.05), $^{\Delta}$indicates there is a difference compared with the model group (P<0.05), $^{\triangledown}$indicates there is a difference compared with the experimental group (P<0.05), and $^{\blacktriangle}$indicates there a difference compared with the blank group (P<0.05).

Table 4. The expressions of the TLR4, CaMKII, Bcl-2, and Bax proteins in liver tissue

Group	TLR4	CaMKII	Bcl-2	Bax	caspase-3
Normal group (n=7)	0.310±0.085	0.302±0.069	1.225±0.184	0.511±0.084	1.147±0.165
Sham operation group (n=7)	0.321±0.080	0.320±0.074	1.208±0.195	0.525±0.095	1.184±0.174
Model group (n=7)	0.841±0.187*	0.811±0.199*	0.508±0.125*	1.148±0.188*	0.635±0.105*
Experimental group (n=7)	0.635±0.159$^{*,\#}$	0.645±0.148$^{*,\#}$	0.699±0.133$^{*,\#}$	0.825±0.122$^{*,\#}$	0.794±0.104$^{*,\#}$
Blank group (n=7)	0.626±0.148$^{*,\#,\Delta}$	0.632±0.158$^{*,\#,\Delta}$	0.705±0.168$^{*,\#,\Delta}$	0.861±0.135$^{*,\#,\Delta}$	0.805±0.118$^{*,\#,\Delta}$
Overexpression group (n=7)	0.468±0.101$^{*,\#,\Delta,\triangledown,\blacktriangle}$	0.468±0.108$^{*,\#,\Delta,\triangledown,\blacktriangle}$	0.925±0.175$^{*,\#,\Delta,\triangledown,\blacktriangle}$	0.669±0.108$^{*,\#,\Delta,\triangledown,\blacktriangle}$	0.938±0.104$^{*,\#,\Delta,\triangledown,\blacktriangle}$
F value	16.878	15.698	22.038	25.358	18.710
P value	<0.001	<0.001	<0.001	<0.001	0.001

Note: *indicates there is a difference compared with the normal group (P<0.05), # indicates there is a difference compared with the sham operation group (P<0.05), $^{\Delta}$indicates there is a difference compared with the model group (P<0.05), $^{\triangledown}$indicates there is a difference compared with the experimental group (P<0.05), and $^{\blacktriangle}$indicates there a difference compared with the blank group (P<0.05).

re significantly different among the groups (P<0.05). There was no difference in the expression of the TLR4, CaMKII, Bcl-2, and Bax proteins between the normal group and the sham operation group (P>0.05). There was no difference in the expressions of the TLR4, CaMKII, Bcl-2 and Bax proteins between the experimental group and the blank group (P>0.05). The expressions of the TLR4, CaMKII and Bax proteins of the normal group and the sham operation group were significantly lower than they were in the model group, the experimental group, the blank group, and the overexpression group, but the Bcl-2 protein expression was just the opposite (P<0.05). The expressions of the TLR4, CaMKII, and Bax proteins in the experimental group and the blank group were significantly lower than they were in the model group, but the Bcl-2 protein expression was just the opposite (P<0.05). The expressions of the TLR4, CaMKII, and Bax proteins of the overexpression group were significantly lower than they were in the model group, the experimental group and the blank group, but the Bcl-2 protein expression was just the opposite (P<0.05) (**Table 4** and **Figure 5**).

The TargetScan target gene prediction and the dual luciferase reporter system

There is a binding site between miR-148a and CaMKII according to the TargetScan database. Through the dual-luciferase reporter system, the luciferase activity of the miR-148a-mimic in the psiCHECK-2-CaMKII-WT group was significantly lower than it was in the unrelated sequence group. There was no significant difference in the luciferase activity of the miR-148a-mimic between the psiCHECK-2-CaMKII-MUT group and the unrelated sequence group (P>0.05) (**Figure 6**).

Discussion

As a very common clinical I/R, liver I/R can be divided into thermal liver I/R and cold I/R according to the type of injury [20]. Among them, thermal I/R is more common in surgical transplantation, shock, and injury. It can induce multiple organ failures in some serious cases. Cold liver I/R is mainly caused by sinusoidal endothelium injury and microcirculatory disorders, which are more common in the preserva-

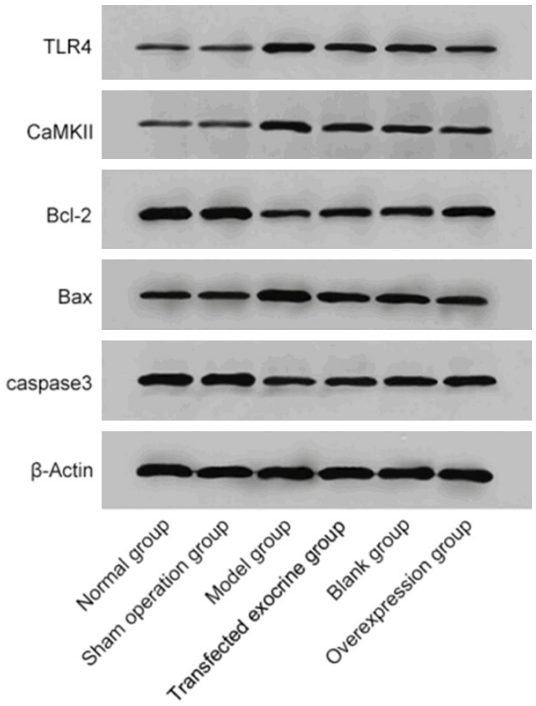

Figure 5. The expressions of the TLR4, CaMKII, Bcl-2, and Bax proteins in liver tissue.

tion stage of the liver in vitro. Although the two I/Rs are caused by different types of damage, they have the same pathological mechanism. How to reduce the occurrence of I/R and hepatocyte apoptosis is one of the urgent problems to be solved.

In recent years, studies have shown that [21] MSC has a significant effect on the treatment of I/R. It is an important cell with multiple differentiation capabilities. Studies of He et al. [22] show that in a cerebral ischemia reperfusion rat model, the transplantation of bone marrow mesenchymal stem cells can inhibit the occurrence of autophagy through the PI3K/Akt pathway. Therefore, the brain can be protected after I/R. In addition, other studies have shown that [23], after the intravenous injection of MSC, certain injured tissue can be repaired. However, after the intravenous injection, a large number of the cells will stagnate in the microcirculation of the lungs. The MSCs that have migrated to the targeted organ are less than 1% of the weight. The survival rate in the host after MSC injection is low, so its effect is limited. Exosomes have maternal cell characteristics. Exosomes are cells that can transmit miR, protein, and regulatory receptor cells [24]. Many studies have shown that [25, 26] exosomes are a new way to communicate among cells, and that exosomes can also protect a variety of cells after they are released from MSCs. In this study, we first observed the protective effect of mesenchymal stem cell exosomes on liver I/R.

As a multifunctional serine/threonine protein kinase, CaMKII plays a major role in regulating the main kinase of Ca^{2+} homeostasis [27]. As an important signal transduction model receptor, the TLR family can promote the occurrence of inflammatory responses, the mature differentiation of immune cells, and the regulation of immune responses [28]. As an important member of the TLR family, studies have shown [29] that TLR4 is involved in the inflammatory response of I/R. In this study, an exosomal solution was injected to the tail vein of the liver I/R rats. It was found that the expressions of TLR4, CaMKII mRNA, and protein in the liver tissue of the model group without the injection of exosomes was significantly increased. The expressions of TLR4, CaMKII mRNA, and proteins of the experimental group with exosomal injection were significantly lower than the expressions in the model group, but higher than of the expressions in the normal group and the sham operation group. We further detected the inflammatory factors IL-1β and TNF-α in the rats' serum. The concentrations of IL-1β and TNF-α in the model group were increased significantly, which was higher than they were in the experimental group. This indicates that the expressions of TLR4, CaMKII, IL-1β, and TNF-α in rat tissues can be effectively reduced by an injection of the exosomal solution. Studies have shown that [30] CaMKII can directly bind to TAK1 and IRF3, and can promote TLR4-mediated inflammatory factors to be released. In addition, there is an inflammatory cascade between them. We speculate that the injection of MSC exosomes may reduce the CaMKII expression in tissues and inhibit the TLR4 signaling pathway. Therefore, the occurrence of the inflammatory response is reduced. Apoptosis is the main mechanism for cell death in I/R. In this experiment, we tested the expression of the Bcl-2 and Bax proteins in rat tissues. Bcl-2 inhibits apoptotic proteins, but Bax promotes apoptotic proteins [27]. By detection, the expression of Bcl-2 proteins in the liver tissue of the model group was significantly de-

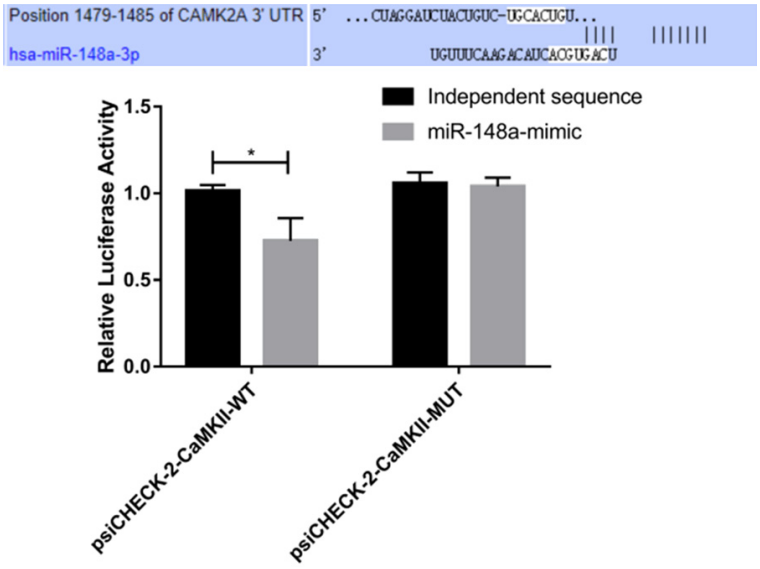

Figure 6. Dual luciferase reporter system. indicates that there is a difference between two groups (P<0.05).

creased and the expression of the Bax protein was significantly increased. In contrast, the expressions of the two proteins in the experimental group were significantly just the opposite. It has been further proved that MSC exosomes can promote the Bcl-2 protein by inhibiting the Bax protein, thereby reducing apoptosis. This study initially demonstrated that the injection of MSC exosomes can reduce CaMKII. TLR4 expression was downregulated. The inflammation response and apoptosis were reduced. But the way to reduce CaMKII is still unclear.

miR has become a popular research topic in recent years. It is a non-coding short interfering RNA with a length of about 19-22 nt, which is highly conserved. It can be bound to target gene 3'-UTRs for regulation of the target gene by complete or incomplete complementary pairing [31]. Studies [18] have shown that there may be a relationship between miR-148a and CaMKII. For this purpose, the miR bound to the CaMKII gene was reversely searched using the TargetScan database. The results showed that there was a targeted binding site between miR-148a and CaMKII. A targeted regulatory function between them was verified through the dual-luciferase reporter system. We further tested the expression of miR-148a in the liver tissues of the experimental group and the model group. The expression of miR-148a in the model group was significantly increased, but the expression of miR-148a in the experimental group was significantly decreased. Both were higher than they were in the normal group and the sham operation group. We speculate that miR-148a may be involved in exosomes, which have increased the expression of miR-148a in tissues and regulates the expression of CaMKII. Therefore, we constructed the miR-148a lentiviral vector miR-148a-mimic and co-transfected it with the exosomes. In the rat liver I/R model with tail vein injection, the miR-148a expression of the overexpression group was significantly higher than it was in the normal group, the sham operation group, the model group, the experimental group, and the blank group. Moreover, the expressions of TLR4, CaMKII mRNA, and protein in the liver tissue of the overexpressing group were significantly lower than they were in the model group and the experimental group. This suggested that the CaMKII expression can be inhibited by over-expressed miR-148a. Furthermore, the expression of TLR4 was decreased, and the expressions of IL-1β and TNF-α in the serum were also significantly lower than they were in the model group and the experimental group. The expression of Bax in the liver tissue of the overexpression group was significantly higher than it was in the model group and the experimental group, but the expression of Bcl-2 was just the opposite. Studies of Wang et al. [32] have shown that oxidized low-density lipoproteins can induce myocardial cell apoptosis in neonatal rats by regulating the TLR4 signaling pathway. In this study, we speculate that inhibition of TLR4 expression can inhibit apoptosis.

In this study, we initially demonstrated that, by intravenously injecting an miR-148a exosomal solution into the liver I/R rat tail, the expressions of CaMKII and TLR4 in liver tissues, the occurrence of the inflammatory response, and the apoptotic process were inhibited. However, there are still some limitations to this study. First, we only tested the rats at one time point.

The expressions of various factors in the liver tissue and serum of the rats at other time points are still unclear. Second, after the inhibition of TLR4 expression, the specific mechanism causing apoptosis is still unclear. Finally, the test is only an animal experiment, and it has not been studied in the clinic. Whether it can be done in the clinic requires further study. Therefore, in future research, we hope to improve the experiment and carry out clinical research to verify the results of our study.

In conclusion, over-expressed miR-148a MSC exosomes can inhibit the expressions of CaMKII and TLR4 in liver I/R tissues and reduce the occurrence of the inflammatory response and apoptosis.

Disclosure of conflict of interest

None.

Address correspondence to: Huihua Cai, Department of Hepatobiliary Surgery, The First People's Hospital of Changzhou, The Third Affiliated Hospital of Soochow University, No. 185, Juqian Street, Changzhou 213000, Jiangsu, China. Tel: +86-15295119918; E-mail: tj19bpo4@163.com

References

[1] Bhogal RH, Weston CJ, Velduis S, G D Leuveninк H, Reynolds GM, Davies S, Nyguet-Thin L, Alfaifi M, Shepard EL, Boteon Y, Wallace L, Oo YH, Adams DH, Mirza DF, Mergental H, Muirhead G, Stephenson BTF and Afford SC. The reactive oxygen species-mitophagy signaling pathway regulates liver endothelial cell survival during ischemia/reperfusion injury. Liver Transpl 2018; 24: 1437-1452.

[2] Olthof PB, van Golen RF, Meijer B, van Beek AA, Bennink RJ, Verheij J, van Gulik TM and Heger M. Warm ischemia time-dependent variation in liver damage, inflammation, and function in hepatic ischemia/reperfusion injury. Biochim Biophys Acta Mol Basis Dis 2017; 1863: 375-385.

[3] Yang X, Li C, Liu J, Liu H, Ma Y, Ng K, Lo C and Man K. IL-17a knockout attenuates inflammatory response and mitochondrial dysfunction after hepatic ischemia-reperfusion injury (Poster Presentation). 2017.

[4] Xie T, Li K, Gong X, Jiang R, Huang W, Chen X, Tie H, Zhou Q, Wu S, Wan J and Wang B. Paeoniflorin protects against liver ischemia/reperfusion injury in mice via inhibiting HMGB1-TLR4 signaling pathway. Phytother Res 2018; 32: 2247-2255.

[5] Aliperta R, Welzel PB, Bergmann R, Freudenberg U, Berndt N, Feldmann A, Arndt C, Koristka S, Stanzione M, Cartellieri M, Ehninger A, Ehninger G7, Werner C, Pietzsch J, Steinbach J, Bornhäuser M and Bachmann MP. Cryogel-supported stem cell factory for customized sustained release of bispecific antibodies for cancer immunotherapy. Sci Rep 2017; 7: 42855.

[6] Crivelli B, Chlapanidas T, Perteghella S, Lucarelli E, Pascucci L, Brini AT, Ferrero I, Marazzi M, Pessina A and Torre ML; Italian Mesenchymal Stem Cell Group (GISM). Mesenchymal stem/stromal cell extracellular vesicles: from active principle to next generation drug delivery system. J Control Release 2017; 262: 104-117.

[7] Sutton MT, Fletcher D, Episalla N, Auster L, Kaur S, Gwin MC, Folz M, Velasquez D, Roy V, van Heeckeren R, Lennon DP, Caplan AI and Bonfield TL. Mesenchymal stem cell soluble mediators and cystic fibrosis. J Stem Cell Res Ther 2017; 7.

[8] Spees JL, Lee RH and Gregory CA. Mechanisms of mesenchymal stem/stromal cell function. Stem Cell Res Ther 2016; 7: 125.

[9] Sun Y, Wang Y, Zhou L, Zou Y, Huang G, Gao G, Ting S, Lei X and Ding X. Spheroid-cultured human umbilical cord-derived mesenchymal stem cells attenuate hepatic ischemia-reperfusion injury in rats. Sci Rep 2018; 8: 2518.

[10] Lee S, Jeong S, Lee C, Oh J and Kim SC. Mesenchymal stem cells derived from human exocrine pancreas spontaneously express pancreas progenitor-cell markers in a cell-passage-dependent manner. Stem Cells Int 2016; 2016: 2142646.

[11] Nugroho WS, Kusindarta DL, Susetya H, Fitriana I, Mulyani GT, Fibrianto YH, Haryanto A and Budipitojo T. The structural and functional recovery of pancreatic beta-cells in type 1 diabetes mellitus induced mesenchymal stem cell-conditioned medium. Vet World 2016; 9: 535-9.

[12] Murtaugh LC and Keefe MD. Regeneration and repair of the exocrine pancreas. Annu Rev Physiol 2015; 77: 229-249.

[13] Nojima H, Freeman CM, Schuster RM, Japtok L, Kleuser B, Edwards MJ, Gulbins E and Lentsch AB. Hepatocyte exosomes mediate liver repair and regeneration via sphingosine-1-phosphate. J Hepatol 2016; 64: 60-68.

[14] Agarwal V, Bell GW, Nam JW and Bartel DP. Predicting effective microRNA target sites in mammalian mRNAs. Elife 2015; 4.

[15] Ding M, Wang C, Lu X, Zhang C, Zhou Z, Chen X, Zhang CY, Ke Z and Zhang C. Comparison of commercial exosome isolation kits for circulating exosomal microRNA profiling. Anal Bioanal Chem 2018; 410: 3805-3814.

[16] Lombard AP, Mooso BA, Libertini SJ, Lim RM, Nakagawa RM, Vidallo KD, Costanzo NC, Ghosh PM and Mudryj M. miR-148a dependent apoptosis of bladder cancer cells is mediated in part by the epigenetic modifier DNMT1. Mol Carcinog 2016; 55: 757-767.

[17] Yang JS, Li BJ, Lu HW, Chen Y, Lu C, Zhu RX, Liu SH, Yi QT, Li J and Song CH. Serum miR-152, miR-148a, miR-148b, and miR-21 as novel biomarkers in non-small cell lung cancer screening. Tumour Biol 2015; 36: 3035-3042.

[18] Zheng D, Li Z, Wei X, Liu R, Shen A, He D, Tang C and Wu Z. Role of miR-148a in mitigating hepatic ischemia-reperfusion injury by repressing the TLR4 signaling pathway via targeting camkiialpha in vivo and in vitro. Cell Physiol Biochem 2018; 49: 2060-2072.

[19] Vila-Petroff M, Salas MA, Said M, Valverde CA, Sapia L, Portiansky E, Hajjar RJ, Kranias EG, Mundina-Weilenmann C and Mattiazzi A. CaMKII inhibition protects against necrosis and apoptosis in irreversible ischemia-reperfusion injury. Cardiovasc Res 2007; 73: 689-698.

[20] Humar A, Kosari K, Sielaff TD, Glessing B, Gomes M, Dietz C, Rosen G, Lake J and Payne WD. Liver regeneration after adult living donor and deceased donor split-liver transplants. Liver Transpl 2010; 10: 1078.

[21] Nong K, Wang W, Niu X, Hu B, Ma C, Bai Y, Wu B, Wang Y and Ai K. Hepatoprotective effect of exosomes from human-induced pluripotent stem cell-derived mesenchymal stromal cells against hepatic ischemia-reperfusion injury in rats. Cytotherapy 2016; 18: 1548-1559.

[22] He H, Zeng Q, Huang G, Lin Y, Lin H, Liu W and Lu P. Bone marrow mesenchymal stem cell transplantation exerts neuroprotective effects following cerebral ischemia/reperfusion injury by inhibiting autophagy via the PI3K/Akt pathway. Brain Res 2019; 1707: 124-132.

[23] Lee RH, Pulin AA, Seo MJ, Kota DJ, Ylostalo J, Larson BL, Semprun-Prieto L, Delafontaine P and Prockop DJ. Intravenous hMSCs improve myocardial infarction in mice because cells embolized in lung are activated to secrete the anti-inflammatory protein TSG-6. Cell Stem Cell 2009; 5: 54-63.

[24] Miyake H, Sakagami J, Yasuda H, Sogame Y, Kato R, Suwa K, Dainaka K, Takata T, Yokota I and Itoh Y. Association of fatty pancreas with pancreatic endocrine and exocrine function. PLoS One 2018; 13: e0209448.

[25] Cao SJ, Wang LF, Ba T, Rong ZD, Hu GL, Zhou B and Li Q. Advances in the research of basic study and clinical application of adipose-derived mesenchymal stem cells. Zhonghua Shao Shang Za Zhi 2018; 33: 184-189.

[26] Lee S, Moon S, Oh JY, Seo EH, Kim YH, Jun E, Shim IK and Kim SC. Enhanced insulin production and reprogramming efficiency of mesenchymal stem cells derived from porcine pancreas using suitable induction medium. Xenotransplantation 2019; 26: e12451.

[27] O'Neill KL, Huang K, Zhang J, Chen Y and Luo X. Inactivation of prosurvival Bcl-2 proteins activates Bax/Bak through the outer mitochondrial membrane. Genes Dev 2016; 30: 973-988.

[28] Alvarado AG and Lathia JD. Taking a toll on self-renewal: TLR-mediated innate immune signaling in stem cells. Trends Neurosci 2016; 39: 463-471.

[29] Tao X, Sun X, Yin L, Han X, Xu L, Qi Y, Xu Y, Li H, Lin Y, Liu K and Peng J. Dioscin ameliorates cerebral ischemia/reperfusion injury through the downregulation of TLR4 signaling via HMGB-1 inhibition. Free Radic Biol Med 2015; 84: 103-115.

[30] Liu X, Yao M, Li N, Wang C, Zheng Y and Cao X. CaMKII promotes TLR-triggered proinflammatory cytokine and type I interferon production by directly binding and activating TAK1 and IRF3 in macrophages. Blood 2008; 112: 4961-4970.

[31] Nguyen TA, Park J, Dang TL, Choi YG and Kim VN. Microprocessor depends on hemin to recognize the apical loop of primary microRNA. Nucleic Acids Res 2018; 46: 5726-5736.

[32] Wang X, Sun Y, Yang H, Lu Y and Li L. Oxidized low-density lipoprotein induces apoptosis in cultured neonatal rat cardiomyocytes by modulating the TLR4/NF-kappaB pathway. Sci Rep 2016; 6: 27866.